JOC*Article*

The Phane Properties of *anti*-[2.2](1,4)Biphenylenophane

Man-kit Leung,* M. Balaji Viswanath, Pi-Tai Chou,* Shih-Chieh Pu, Hsin-Chieh Lin, and Bih-Yaw Jin*

Department of Chemistry, National Taiwan University, Taipei, Taiwan 106

mkleung@ntu.edu.tw

Received December 16, 2004

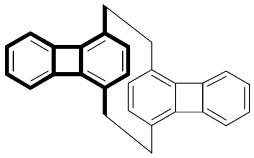

anti-[2.2](1,4)Biphenylenophane (**4**) was synthesized from de Meijere's tetrabromo[2.2]paracyclophane (**5**) through a four-step reaction sequence. Although an average separation of 3.09 Å between the inner ring of the biphenylene units is normal for [2.2]paracyclophanes, a bond distance of 1.54 Å for the ethano C−C bridge at room temperature is shorter than usual. In addition, trimethylsilyl-substituted *anti*-[2.2](1,4)biphenylenophane **8** sublimes at 220 °C under a pressure lower than 1×10^{-5} Torr without decomposition or thermal isomerization. The high thermal stability of **8** suggested that the ethano bridges of the biphenylenophanes are less strained than those of [2.2]paracyclophane. Bathochromic shifts are observed in their UV−vis absorption spectra. The phane state interactions of **4** and **8** were evidenced by the weak structureless fluorescent emission maximized at 537 and 550 nm in CH_2Cl_2 along with longer relaxation lifetimes of 229 and 292 ps, respectively.

Introduction

Understanding the principles of electronic delocalization between proximate nonconjugated π-units is of great importance for designing novel optoelectronic materials.[1] In particular, orientation of π-stacking of aromatic components and $\pi-\pi$ orbital interactions are major factors that control charge mobility of organic materials in condense phase.[2] To mimic a face-to-face π-stacking environment for fundamental studies and applications, [2.2]paracyclophane **1** has been used extensively as a framework to hold π-units in close proximity.[3,4] The constrained geometry of [2.2]paracyclophane results in a 2.8 Å separation between the *ipso*-carbon atoms of the stacked rings and a 3.1 Å separation between the planes of the remaining four unsubstituted aromatic carbon atoms of each ring.[5] The inter-ring spacing is considerably shorter than the 3.4 Å interplanar separation for effective π stacking. Therefore, the photophysical properties and electronic properties of conjugated derivatives of [2.2]paracyclophane are of particular interest to research.

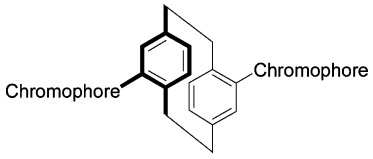

1

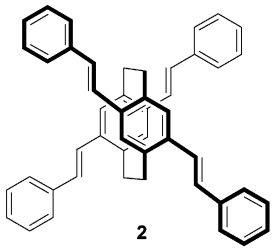

2

example of criss-cross chromophore

Recently, the concepts of phane-state delocalization have been introduced to explain the structureless emission behavior of some particular [2.2]paracyclophanes.[3a,b] In addition, the HOMO−LUMO density of the conjugated fragments was found to be an important factor that governs the phane-state interactions. For examples, criss-cross chromophore **2** allows overlap of the central rings that participate strongly in the HOMO and the LUMO, leading to a strong orbital mixing in the phane state that is delocalized across the entire molecule.[3b]

(1) (a) Pope, M.; Swenberg, C. E. *Electronic Processes in Organic Crystals and Polymers*; Oxford: New York, 1999. (b) Garnier, F. *Acc. Chem. Res.* **1999**, *32*, 209−215. (c) Tolbert, L. M. *Acc. Chem. Res.* **1992**, *25*, 561−568.

(2) (a) Cornil, J.; Beljonne, D.; Calbert, J.-P.; Bredas, J.-L. *Adv. Mater.* **2001**, *13*, 1053−1067. (b) Kaikawa, T.; Takimiya, K.; Aso, Y.; Otsubo, T. *Org. Lett.* **2000**, *2*, 4197−4199. (c) Miller, L. L.; Mann, K. R. *Acc. Chem. Res*. **1996**, *29*, 417−423.

10.1021/jo047802n CCC: $30.25
Published on Web 04/06/2005

π-Systems having antiaromatic characters have been important topics for research throughout the last few decades.[6] Due to the small HOMO−LUMO energy gap, antiaromatic compounds are, in principle, highly polarizable and would show strong intermolecular interactions.[7] However, antiaromatic compounds are usually reactive, and hence, examples of stable antiaromatic compounds are rare. Most of the cyclic 4n systems are structurally distorted so as to avoid antiaromaticity. Biphenylene and [*N*]phenylenes attract the interest of chemists because they are considered a family of thermodynamically stable cyclic 4n compounds.[8,9] In comparison to biphenyl, biphenylene has a relatively small HOMO−LUMO gap, low oxidation, and reduction potentials.[10] The higher homologues of biphenylene, known as [*N*]-phenylenes, are predicted by MO theory to have progressively smaller difference in energy between their HOMOs and LUMOs.[11] Therefore, we are interested in combining the concept of phane-state delocalization and [*N*]-phenylenes antiaromaticity to create novel π systems.

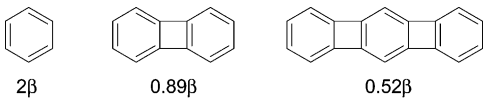

HOMO-LUMO energy differences

$\pi-\pi$ orbital interactions between biphenylene units were evaluated in the 1970s. Face-to face-biphenylenophane **3** was synthesized, and its photophysical properties were investigated.[12] Based on the chemical shifts of the benzenoid protons, a cross-overlapped structure of **3** was concluded. As our interest in biphenylene chemistry continues,[13] we report herein the synthesis and the physical properties of [2.2](1,4)biphenylenophane (**4**).

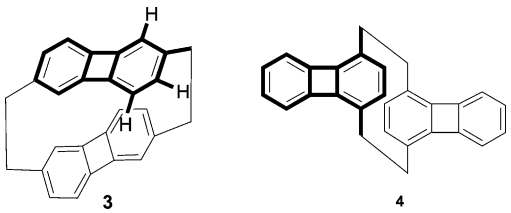

3 **4**

Results and Discussion

Synthesis of the Cyclophanes. Biphenylenophane **4** was synthesized from de Meijere's tetrabromide[3k] **5** in four steps (Scheme 1). The first attempt of acetylenation of **5** with trimethylsilylacetylene using copper-catalyzed Sonogashira coupling conditions was unsuccessful.[14] After attempts under various conditions, we concluded that the $ZnCl_2$-promoted procedure is the most effective approach to convert **5** to **6**.[15] Desilylation of **6** using TBAF to give **7**, followed by Vollhartd's biphenylene synthesis, gives tetrasilylated product **8** in 34% yield.[11] Although the yield of this step is not particularly high, it is reasonable because two biphenylene units were substantially formed in one pot. Attempts of removal of the trimethylsilyl groups either in trifluoroacetic acid (TFA) or in the

(3) For recent reviews, see: (a) Hong, J. W.; Benmansour, H.; Bazan, G. C. *Chem. Eur. J.* **2003**, 9, 3186−3192. (b) Bartholomew, G. P.; Bazan, G. C. *Acc. Chem. Res.* **2001**, *34*, 30−39. For recent related literature, see: (c) Grimme, S. *Chem. Eur. J.* **2004**, *10*, 3423−3429. (d) Lyssenko, K. A.; Yu, Antipin. M. Y.; Yu. Antonov, D. *ChemPhysChem* **2003**, *4*, 817−823. (e) Salhi, F.; Lee, B.; Metz, C.; Bottomley, L. A.; Collard, D. M. *Org. Lett.* **2002**, *4*, 3195−3198. (f) Bartholomew, G. P.; Ledoux, I.; Mukamel, S.; Bazan, G. C.; Zyss, J. *J. Am. Chem. Soc.* **2002**, *124*, 13480−13485. (g) Hong, J. W.; Gaylord, B. S.; Bazan, G. C. *J. Am. Chem. Soc.* **2002**, *124*, 11868−11869. (h) Moran, A. M.; Bartholomew, G. P.; Bazan, G. C.; Kelley, A. M. *J. Phys. Chem. A* **2002**, *106,* 4928−4937. (i) Bodwell, G. J.; Miller, D. O.; Vermeij, R. J. *Org. Lett.* **2001**, *3*, 2093−2096. (j) Wang, S.; Bazan, G. C.; Tretiak, S.; Mukamel, S. *J. Am. Chem. Soc.* **2000**, *122*, 1289−1297. (k) Zyss, J.; Ledoux, I.; Volkov, S.; Chernyak, V.; Mukamel, S.; Bartholomew, G. P.; Bazan. G. C. *J. Am. Chem. Soc.* **2000**, *122,* 11956−11962. (l) Konig, B.; Knieriem, B.; de Meijere, A. *Chem. Ber.* **1993**, *126*, 1643. (m) Reiser, O.; Koenig, B.; Meerholz, K.; Heinze, J.; Wellauer, T.; Gerson, F.; Frim, R.; Rabinovitz, M.; de Meijere, A. *J. Am. Chem. Soc.* **1993**, *115*, 3511−3518.

(4) For application of phane interactions to polymeric materials, see: (a) Morisaki, Y.; Chujo, Y. *Macromolecules* **2003**, *36*, 9319−9324. (b) Morisaki, Y.; Fujimura, F.; Chujo, Y. *Organometallics* **2003**, *22*, 3553−3557. (c) Morisaki, Y.; Ishida, T.; Chujo, Y. *Macromolecules* **2002**, *35*, 7872−7877. (d) Morisaki, Y.; Chujo, Y. *Chem. Lett.* **2002**, 194−195. (e) Morisaki, Y.; Chujo, Y. *Macromolecules* **2002**, *35*, 587−589. (f) Salhi, F.; Collard, D. *Polym. Mater. Sci. Eng.* **2002**, *86*, 222. (g) Popova, E. L.; Rozenberg, V. I.; Starikova, Z. A.; Keuker-Baumann, S.; Kitzerow, H.-S.; Hopf, H. *Angew. Chem., Int. Ed.* **2002**, *41*, 3411−3414. (h) Guyard, L.; Audebert, P. *Electrochem. Commun.* **2001**, *3*, 164−167. (i) Guyard, L.; Nguyen Dinh, An. M.; Audebert, P. *Adv. Mater.* **2001**, *13*, 133−136. (j) Collard, D. M.; Lee, B. *Polym. Prepr.* (*Am. Chem. Soc., Div. Polym. Chem.*) **2000**, *41*, 241. (k) Mizogami, S.; Yoshimura, S. *J. Chem. Soc., Chem. Commun.* **1985**, 1736−1738.

(5) For current reviews of [2.2]paracyclophanes, see: (a) Nishimura, J.; Nakamura, Y.; Hayashida, Y.; Kudo, T. *Acc. Chem. Soc.* **2000**, *33*, 679−686. (b) Shultz, J.; Vögtle, F. *Top. Curr. Chem.* **1994**, *172*, 42. (c) Vögtle, F. *Cyclophane Chemistry*; Wiley & Sons: New York, 1993. (d) Diederich, F. *Cyclophanes*; Royal Society of Chemistry: Cambridge, 1991.

(6) (a) Garratt, P. J. *Aromaticity*; Wiley: Maidenhead, U.K., 1986. (b) Minkin, V. I.; Glukhotsev, M. N.; Simkin, B. Ya. *Aromaticity and Antiaromaticity: Electronic and Structural Aspects*; Wiley: New York, 1994. (c) Wiberg, K. B. *Chem. Rev.* **2001**, *101*, 1317−1332. (d) Maier, G. *Angew. Chem., Int. Ed. Engl.* **1988**, *27*, 309−332. (e) Bally, T.; Masamune, S. *Tetrahedron* **1980**, *36*, 343−370. (f) Maier, G. *Angew. Chem., Int. Ed. Engl.* **1974**, *13*, 425−490. (g) Breslow, R. *Acc. Chem. Res.* **1973**, *6*, 393−398.

(7) Chattaraj, P. K. *J. Phys. Chem. A* **2001**, *105,* 511−513 and references therein.

(8) For reviews, see: (a) Shephard, M. K. *Cyclobutarenes*; Elsevier: Amsterdam, 1991. (b) Toda, F.; Garratt, P. *Chem. Rev.* **1992**, *92*, 1685−1707.

(9) (a) Kumaraswamy, S., Jalisatgi, S. S.; Matzger, A. J.; Miljanić, O. Š.; Vollhardt, K. P. C. *Angew. Chem., Int. Ed.* **2004**, *43*, 3711−3715. (b) Iglesias, B.; Cobas, A.; Pérez, D.; Guitián, E.; Vollhardt, K. P. C. *Org. Lett*. **2004**, *6*, 3557−3560 (c) Bong, D. T.-Y.; Chan, E. W. L.; Diercks, R.; Dosa, P. I.; Haley, M. M.; Matzger, A. J.; Miljanic, O. S.; Vollhardt, K. P. C.; Bond, A. W.; Teat, S. J.; Stanger, A. *Org. Lett.* **2004**, *6*, 2249−2252. (d) Bruns, D.; Miura, H.; Vollhardt, K. P. C. Stanger, A. *Org. Lett.* **2003**, *5*, 549−552. (e) Bong, D. T.-Y.; Gentric, L.; Holmes, D.; Matzger, A. J.; Scherhag, F.; Vollhardt, K. P. C. *Chem. Commun.* **2002**, 278−279. (f) Eickmeier, C.; Holmes, D.; Junga, H.; Matzger, A. J.; Scherhag, F.; Shim, M.; Vollhardt, K. P. C. *Angew. Chem., Int. Ed.* **1999**, *38*, 800−804. (g) Holmes, D.; Kumaraswamy, S.; Matzger, A. J.; Vollhardt, K. P. C. *Chem. Eur. J.* **1999**, *5*, 3399−3412.

(10) (a) Olah, G. A.; Liang, G. *J. Am. Chem. Soc.* **1976**, *98*, 3033−3034, **1977**, *99*, 6045−6049. (b) Ronlan, A.; Parker, V. D. *J. Chem. Soc., Chem. Commun.* **1974**, 33. (c) Bauld, N. C.; Banks, D. *J. Am. Chem. Soc.* **1965**, *87*, 128−129. (d) Waack, R.; Doran, M. A.; West, P. *J. Am. Chem. Soc.* **1965**, *87*, 5508−5510.

(11) (a) Dosche, C.; Löhmannsröben, H.-G.; Bieser, A.; Dosa, P. I.; Han, S.; Iwamoto, M. Schleifenbaum. A.; Vollhardt, K. P. C. *Phys. Chem. Chem. Phys.* **2002**, *4*, 2156−2161. (b) Berris, B. C.; Hovakeemian, G. H.; Lai, Y.-H.; Mestdagh, H.; Vollhardt, K. P. C. *J. Am. Chem. Soc.* **1985**, *107*, 5670−5687. (c) Berris, B. C.; Lai, V.-H.; Vollhardt, K. P. C. *J. Chem. Soc., Chem. Commun.* **1982**, 953−954.

(12) Sato, M.; Ueno, H.; Ogawa, T.; Ebine, S. *Tetrahedron Lett.* **1984**, *25*, 3603−3606.

(13) (a) Lin, S.-C.; Chen, J.-A.; Liu, M.-H.; Su, Y. O.; Leung, M.-K. *J. Org. Chem.* **1998**, *63*, 5059−5063. (b) Kwong, C.-Y.; Chan, T.-L.; Chow, H.-F.; Lin, S.-C.; Leung, M.-k. *J. Chin. Chem. Soc.* **1997**, *44*, 211−224. (c) Kwong, C.-Y.; Leung, M.-k.; Lin, S.-C.; Chan, T.-L.; Chow, H.-F. *Tetrahedron Lett.* **1996**, *37*, 5913−5916.

(14) (a) Diercks, R.; Armstrong, J. C.; Boese, R.; Vollhardt, K. P. C. *Angew. Chem., Int. Ed. Engl.* **1986**, *25*, 268−269.

(15) (a) Negishi, E.; Qian, M.; Zeng, F.; Anastasia, L.; Babinski, D. *Org. Lett.* **2003**, *5*, 1597. (b) King, A. O.; Negishi, E.; Villani, F. J., Jr.; Silveira, A., Jr. *J. Org. Chem.* **1978**, *43*, 358−360.

TABLE 1. Comparison of C−C and C=C Bond Lengths of the Outside Ring

	C=C bond lengths (Å)	average	C−C bond lengths (Å)	average
4	1.364, 1.368, 1.358	1.363 ± 0.005	1.409, 1.403, 1.409	1.407 ± 0.004
10	1.385, 1.372, 1.372	1.376 ± 0.008	1.423, 1.423, 1.426	1.424 ± 0.002
11	1.370, 1.365, 1.369	1.368 ± 0.003	1.404, 1.400, 1.413	1.406 ± 0.007

SCHEME 1

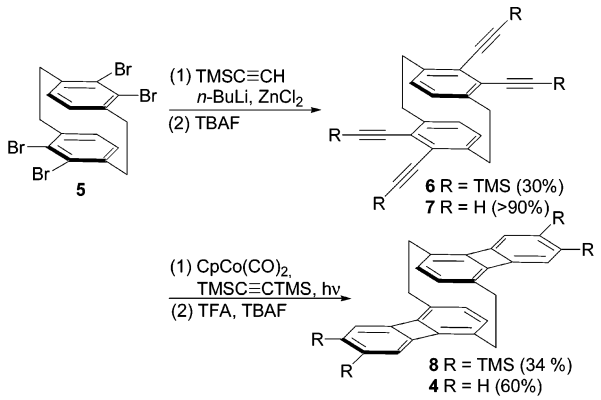

presence of tetrabutylammonium fluoride (TBAF) alone was unsuccessful.[16] However, the trimethylsilyl (TMS) groups could be successfully removed by TBAF in TFA to afford **4** as slightly yellowish needles.

X-ray Crystallographic Analysis. Single crystals were prepared by slow evaporation of a solution of **4** in CH_2Cl_2/MeOH (1:1). The constitution of **4** has been verified by X-ray crystallographic analysis, and their C−C bond lengths are summarized in Figure 1. The single crystal of **4** is *Pbca* with Z = 4, $R(F_o)(I > 2\sigma(I)) = 0.0525$, and $R(F_o)$(all data) = 0.131. Two biphenylene units of **4** are aligned in an anti-form. In the crystal lattice, the torsional angle of 2.9° within the ethano bridge is smaller than that of substituted [2.2]paracyclophanes, in which the torisonal angles are reported around 14−22°.[3k] Due to ring strain of the cyclophane skeleton, the central benzenoid rings are bent into boatlike structure so that the six aromatic carbon atoms are no longer displaced on the same plane. On the contrary, the outside benzenoid rings are planar but tilted slightly inward as seen from the side view. In the central rings, the average bond length of the C=C bonds is 1.364 Å and the average bond length of the C−C bonds is 1.426 Å. Their difference is 0.062 Å. In the outside rings, the average bond length of the C=C bonds is 1.363 Å and the average bond length of the C−C bonds is 1.408 Å. Their difference is 0.045 Å. A large C−C/C=C difference in the central benzenoid rings implies that the π bonds are more localized in comparison to the outside ring and are more similar to cyclohexatriene.

The outside six-membered rings are geometrically more regular. Either the C−C single bonds or the C=C double bonds have similar bond lengths (Table 1). The C=C bond lengths of 1.364(4), 1.368(3), and 1.358(3) Å and the C−C bond lengths of 1.409(3), 1.403(4), and 1.409(4) Å are somewhat shorter than that of biphenylene (**10**)[17] but geometrically close to the outside rings of **11**.[18] It has been reported that [3]phenylene (**11**) minimizes cyclic 4n destabilization through strong bond localization

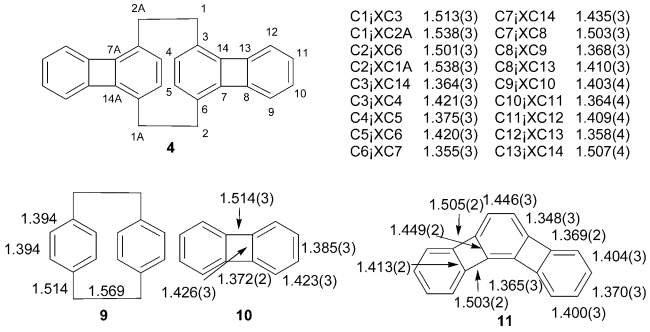

FIGURE 1. Carbon−carbon bond lengths of **4** and **9**−**11**.

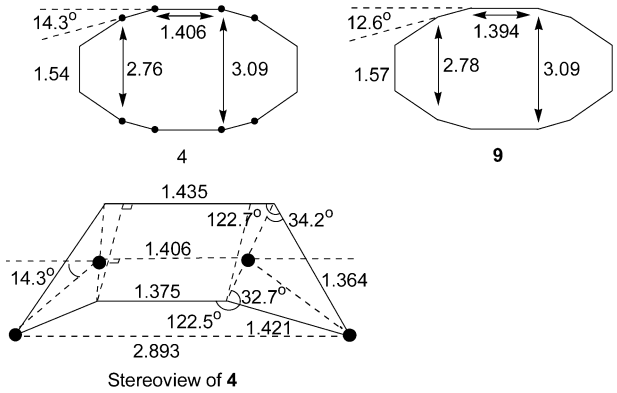

FIGURE 2. Schematic diagrams for the profiles of **4** and **9** (at 93 K)**.** Black dots in **4** indicate the location of the profile.

of the central ring, accompanied by higher degree of delocalization of the outer ring. As we mentioned above, the central rings of **4** are bent and have obvious bond localization phenomenon, in particular with an unusually long C_7-C_{14} bond of 1.435(3) Å. This may reduce the antiaromatic effects of the central cyclobutadiene circuits and therefore enhance the delocalization of the outside rings.[19]

Another interesting feature about the family of [2.2]-paracyclophanes is the inter-ring spacing between the facing aromatic ring.[20] Figure 2 shows the schematic diagrams for the carbon skeleton profiles of **9** and the central part of **4**. The distal lengths between C_4-C_{7A} and C_5-C_{14A} of **4** are 3.088 and 3.102 Å, respectively. An average of 3.09 Å between the facing planes is identical with that of **9**. This distance is short enough to allow significant $\pi-\pi$ orbital interactions between two facing

(16) Iyer, V. S.; Yoshimura, K.; Enkelmann, V.; Epsch, R.; Rabe, J. P.; Müllen, K. *Angew. Chem., Int. Ed.* **1998**, *37*, 2696−2699.

(17) Fawcett, J. K.; Trotter, J. *Acta Crystallogr.* **1966**, *20*, 87−93.

(18) Diercks, R.; Vollhardt, K. P. C. *Angew. Chem., Int. Ed. Engl.* **1986**, *25*, 266−268.

(19) For discussions of the effect of the central cyclobutadiene circuits, see: (a) Hess, B. A.; Schaad, L. J. *J. Am. Chem. Soc.* **1971**, *93*, 305−310. (b) Glidewell, C.; Loyd, D. L. *Chem. Script.* **1986**, *26*, 623. (c) Vogtle, F.; Saitmacher, K.; Peyerimhoff, S.; Hippe, D.; Puff, H.; Bullesbach, P. *Angew. Chem., Int. Ed. Engl.* **1987**, *26*, 470. (d) Reference 7, p 21.

(20) Hope, H.; Bernstein, J.; Trueblood, K. N. *Acta Crystallogr.* **1972**, *B28*, 1733−1743.

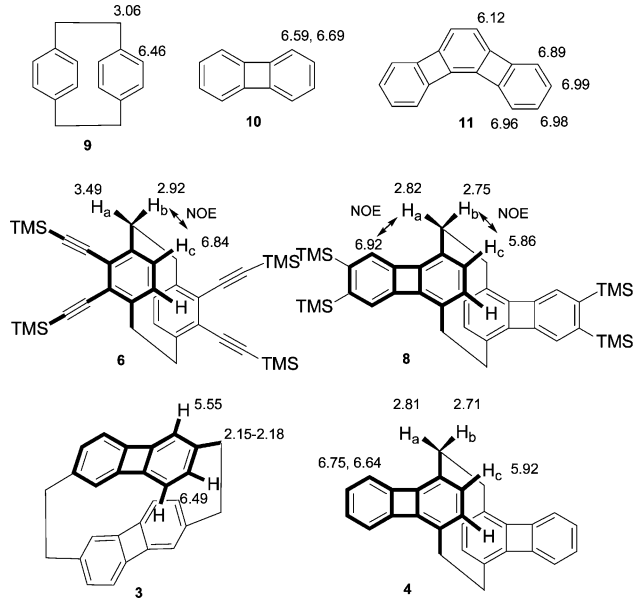

FIGURE 3. Chemical shifts of **3**, **4**, **6**, and **8**−**11**.

units. However, the degree of deformation of the central six-membered rings into a boatlike structure is slightly larger than **9**. The *ipso*-carbon atoms C_3 and C_6 are bent about 14.3° out of the plane of C_4, C_5, C_7, and C_{14}. In addition, the ethano C−C bond length of 1.538(3) Å at room temperature is close to that of 1.56 Å for **9** at 93 K but shorter than that of 1.63 Å at room temperature.[21] This implies that the less aromatic 12π electron biphenylene units could be more easily deformed than the benzene ring in **9**. Strains of biphenylene originate from angle distortion, a 4n array of the central cyclobutadiene ring, and bond localization of the benzenoid rings. Strain energies arising from bending of the central benzenoid rings could be partially compensated by reduction of the antiaromatic cyclobutadiene character and enhancing the degree of bond delocalization in the outside benzenoid rings. Therefore, the strains on the ethano bridges are less and hence the degree of elongation of the C−C bond at room temperature is less.

^{1}H NMR Analysis. The ^{1}H NMR data are summarized in Figure 3. In comparison to the ^{1}H NMR spectrum of biphenylene in which the benzenoid protons resonate as an AA′BB′ system centered at δ 6.69 and 6.59 ppm,[22] **4** exhibits a remarkably shielded singlet in $CDCl_3$ for the central benzenoid hydrogens at δ 5.92, along with the two signals for the AA′BB′ system centered at 6.75 and 6.64 ppm. Although the shielding effects may originate from the paratropic current of the facing biphenylene units, π-bond localization effects on the central rings that reduce the diatropism may also contribute to the upfield shift. The resonance chemical shift of 5.92 ppm is still within the region of normal vinylic protons, such as δ =5.8−5.9 for 1,3-cyclohexadiene.[23]

(21) See ref 5c, p 76.

(22) (a) Andres, W.; Günther, H.; Günther, M.-E.; Hausmann, H.;. Jikeli, G.; von Puttkamer, H.; Schmickler, H.; Niu-Schwarz, J.; Schwarz W. H. E. *Helv. Chim. Acta* **2001**, *84*, 1737−1755. (b) Günther, H.; Jikeli, G.; Schmickler, H.; Prestien, J. *Angew. Chem., Int. Ed. Engl.* **1973**, *12*, 762−763.

(23) Pretsch, E.; Seibl, J.; Simon, W.; Clerc, T. *Tables of Spectral Data for Structure Determination of Organic Compounds*, 2nd ed.; Springer: Berlin, 1989; p H235.

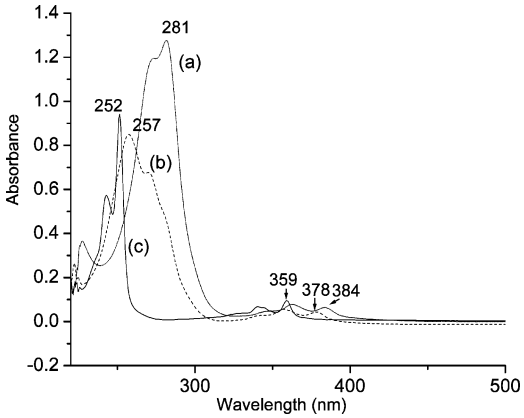

FIGURE 4. UV−vis absorption spectra of (a) **8**, (b) **4**, and (c) **10**.

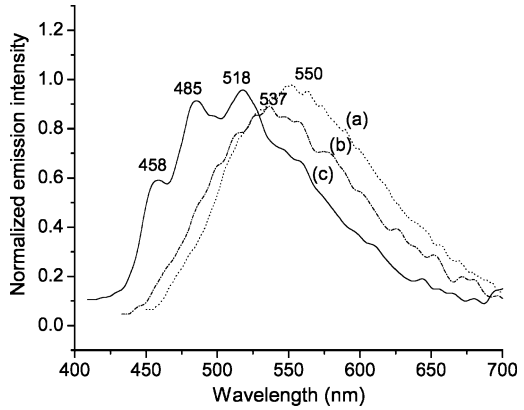

FIGURE 5. Fluorescent spectra of (a) **8**, (b) **4**, and (c) **10**. Note that in order to show the spectral profiles, the original spectral data were treated by the Savitzky Golay polynomial method for noise reduction.

Shielding effects are also observed for the ethano protons. The assignments of the chemical shifts are established on the basis of the NOE between the inner ethano protons H_b and the central *aromatic* protons H_c. Prior to the biphenylene formation, the outer methylene protons H_a of the diacetylenic precursor **6** are highly deshielded to δ 3.49. We attributed this to the diatropic ring current effects of the acetylene units. However, perhaps due to the paratropic ring current effects of the biphenylene units, the H_a of **8** are upfield shifted by nearly 0.67 ppm to δ 2.82 ppm. This value is upfield even in comparison to that of [2.2]paracyclophane (**9**) by 0.23 ppm. Nevertheless, the shielding effect is not as remarkable as in **3**, in which the methylene proton resonance signals at δ = 2.15−2.18 ppm.[11]

Photophysical Properties. Since the biphenylene units of **4** and **8** are arranged in a half-overlap position with sufficiently rigid conformation, we expect **4** and **8** to be intriguing from a photophysical point of view. Electronic coupling between two facing biphenylene units is evident in both the absorption and fluorescent spectra (Figures 4 and 5). The UV−vis spectra of **4**, **8**, and **10** contain two major bands at the regions of 200−300 nm and 310−400 nm. In comparison to **10**, the spectral broadening and bathochromic shift of the absorption

bands of **4** and **8**[24] indicate significant ground-state transannular interactions between the biphenylene units. Similar to the spectrum of biphenylene, weak absorption bands between 330 and 400 nm are attributed to the symmetry forbidden electronic transitions while the group of absorption bands at 250−300 nm corresponds to the symmetry allowed electronic transitions. These assignments are in sound agreement with the results of semiempirical calculation in which the PM3/RHF method was employed for structural optimization and the ZINDO method for spectral calculation. For **4** and **8**, the lowest energy absorption bands shifted by 1400 and 1810 cm^{-1}, respectively, to 378 and 384 nm.

A detailed explanation for the spectral data of **4** and **8** requires more complicated quantum mechanical analysis. In particular, the presence of degenerated or near-degenerated π-molecules in biphenylene makes the spectral assignment complicated. Nevertheless, it has been reported that the lowest energy electronic transitions of biphenylene **10** are also symmetry forbidden.[11a,25] This is consistent with the observation of weak absorption bands in 330−400 nm in our case. A similar bathochromic shift was also reported for **3** in the previous literature. A more in-depth discussion on the spectral data will be presented in a later section for theoretical consideration.

In contrast to the photoluminescent behavior of biphenylene, fluorescence spectra of **4** and **8** showed structureless excimer-like green emission peaking at 537 and 550 nm, respectively (Figure 5). Since the photoluminescence intensity is weak, the origin of the fluorescence spectra was confirmed by their identical excitation and absorption spectra. Although the diffusive emission behavior is one of the basic characters for "phane" state delocalization that is somewhat similar to excimer emission,[3a,b] the Stokes shifts (peak to peak) of about 160 nm that were observed for **4** or **8** are nearly identical to that of **10**. This leads to a question of whether the emission is mainly arising from the biphenylene units or from the core of the phane unit. Longer fluorescence lifetime with weak emission intensity is another special character of the phane state emission. In the present cases, longer fluorescent lifetimes were also observed for **4** and **8**. While the lifetime of the authentic biphenylene in dichloromethane (concentrated 30 μM) is 194 ps,[25] it was found to be 229 and 292 ps for **4** and **8,** respectively. These observations suggested that the phane-state interactions should have a certain extent of contribution to the emission spectra of **4** and **8**.

These observations could be well explained by Bazan's theory on phane-state interactions, a theory established for explaining three-dimensional electronic delocalization within paracyclophane based bichromophores (Scheme 2). When the paracyclophane core acts as a bridge to bring two individual chromophores into close contact, permanent chromophore−chromophore through-space delocalization is established in a well-defined way. The photophysical properties of the paracyclophane bichromophores derive mainly from two states: the chromophore state and the phane state. In the present case, the chromophore states are derived from through bond (TB) interactions within the biphenylene units. On the other hand, electronic delocalization across the paracyclophane occurs via the through-space (TS) phane-state interactions. According to the results from previous literature,[3] we expected that the energy level of the TS phane interactions should be lie much higher than the lowest excited states of the biphenylene units. In this circumstance, mixing of the phane state and the lowest chromophoric excited states should be small. Therefore, the lowest excited states of **4** and **8** can be described as mostly the biphenylene in character. However, the corresponding spectral behavior would be modified to a certain extent by the phane properties. This prediction is in good agreement with the observation of small red shifts on the absorption spectra of **4** and **8**, as well as the diffusive fluorescent emission. In addition, due to a smaller gap between the phane state and the higher biphenylene excited states, stronger mixing of the states is expected. This could rationalize the larger extent of spectral shift on the higher energy absorption bands at around 250 nm. Since we are interested in further understanding the electronic interactions within **4**, a theoretical model was built to mimic **4** as follows.

SCHEME 2

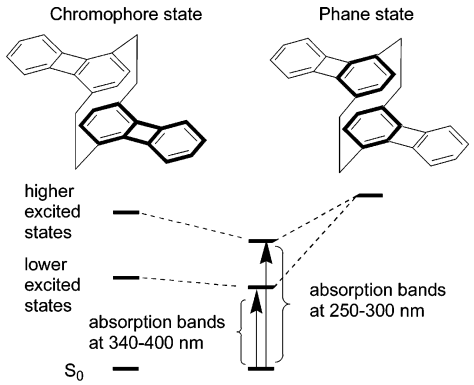

Theoretical Aspects for the Photophysical Properties. The measurement and interpretation of the electronic spectra of biphenylene have been extensively studied throughout last few decades. In our theoretical treatment, we mimic the electronic properties of **4** by a model with two biphenylene units in close contact. The ground-state geometry of the biphenylene monomer is optimized by means of the semiempirical Hartree−Fock Austin model 1 (AM1) method.[26] On the basis of the optimized biphenylene geometry, we compute excited-state properties of the cofacial (H-type) and head-to-tail (J-type) dimers by Molecule-in−molecule (MIM) Hamiltonian[27] via Pariser−Parr−Pople (PPP) Hamiltonian[28] coupled to a single configuration-interaction (SCI) scheme with all occupied and unoccupied π-levels. The stackings

(24) (a) Yatsuhashi, T.; Akiho, T.; Nakashima, N. *J. Am. Chem. Soc.* **2001**, *123*, 10137−10138. (b) Lin, H. B.; Topp, M. *Chem. Phys. Lett.* **1979**, *64*, 452−456. (c) Garratt, P. J.; Vollhardt, K. P. C. *J. Am. Chem. Soc.* **1972**, *94*, 7087−7092.

(25) A half-life of 238 ps for biphenylene was reported in the literature in cyclohexane with a quantum yield of 1.7×10^{-4}. For reference, see: Suarez, M.; Devadoss, C.; Schuster, G. B. *J. Phys. Chem.* **1993**, *97*, 9299−9303.

(26) The geometry of the biphenylene was optimized by AM1 with a calculated total energy of 120.22 kcal/mol. For reference, see: Dewar, M. J. S.; Zoebisch, E. G.; Healy, E. F.; Stewart, J. J. P. *J. Am. Chem. Soc.* **1985**, *107*, 3902.

(27) Longuet-Higgins, H. C.; Murrell, J. N. *Proc. Phys. Soc. A.* **1955**, *68*, 601.

(28) Pople, J. A.; Beveridge, D. L. *Approximate Molecular Orbital Theory*; McGraw-Hill: New York, 1970.

of the biphenylene units in the form of *H*-aggregation and in the form of *J*-aggregation are then compared.

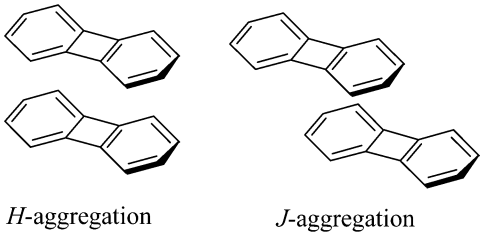

The nature of electronic excited states of cyclophane consisting of two cyclic π-electron systems derived from a 4N-electron perimeter is quite different from those systems based on a (4N + 2)-electron perimeter. To explore the effect of the transannular interaction on the most important low-lying electronic excited states, particularly, the relative weights of local exciton and charge-transfer exciton, we have adopted the composite-molecule method of Longuet−Higgins and Murrel[27] to perform configuration interaction. The usual supermolecular calculation treats the two moieties in the phane as a single quantum system; therefore, the important details concerning the charge-transfer cannot be achieved in a straightforward way. The composite-molecule method is based on the local molecular orbitals and the excited-state wave function of cyclophane is expressed in terms of a superposition of a local exciton and charge resonance configurations

$$\Psi_{\pm} = \sum_i c^{\mathrm{ex}}_{\pm,i} 1/\sqrt{2}(L^*_i R_0 \pm L_0 R^*_i) + \sum_{a,r} c^{\mathrm{ct}}_{\pm,ar} 1/\sqrt{2}(L^*_a R^-_r \pm L^-_r R^*_i)$$

where $L^*_i(R^*_i)$ is the i-th singlet state of monomer L(R) and $L^+_a R^-_r(L^-_r R^+_a)$ corresponds to a charge-transfer (CT) configuration in which an electron moves from local molecular orbital φ_a of molecule L (R) to unoccupied orbital φ_r of molecule R (L). The percentage of exciton resonance component and charge resonance component can be calculated

$$w_{\mathrm{LE}} = \sum_i |c^{\mathrm{ex}}_i|^2$$

$$w_{\mathrm{CT}} = \sum_{ar} |c^{\mathrm{ct}}_{ar}|^2$$

for which $w_{\mathrm{LE}} + w_{\mathrm{CT}} = 100\%$. Therefore, the relative weights w_{LE} and w_{CT} stand for a useful measure of transannular interaction for the two moieties in a cyclophane, which is hard to obtain from a supermolecular approach commonly used by many researchers.

Our composite-molecule calculation is based on the standard PPP model. This model has recently been shown to reproduce low-lying singly excited states pretty well.[29] Two types of biphenylene cyclophanes and their face-to-face (H-aggregation) and head-to-tail (J-aggregation) arrangements are investigated in the present paper. The perpendicular distance between two plarnar biphenylenes is chosen to be within 3.0−4.5 Å. For a qualitative discussion, only a situation with d = 4.0 Å is reported. A detailed investigation on the distance dependence will be presented later. To facilitate the discussion, we show a schematic diagram of six local perimeter molecular orbitals and the corresponding energy diagram of a monomeric biphenylene in Figure 6. There are two types of electronic excitations: those excitations involve the creation of local exciton and those configurations with charge transfer between two moieties in the cyclophane. The notation and classification of molecular orbitals and electronic states closely follow the perimeter labels proposed by Fleischhauer et al.[29] Only five (out of 10) essential local exciton states and five (out of 10) charge-transfer configurations are shown in Figure 6.

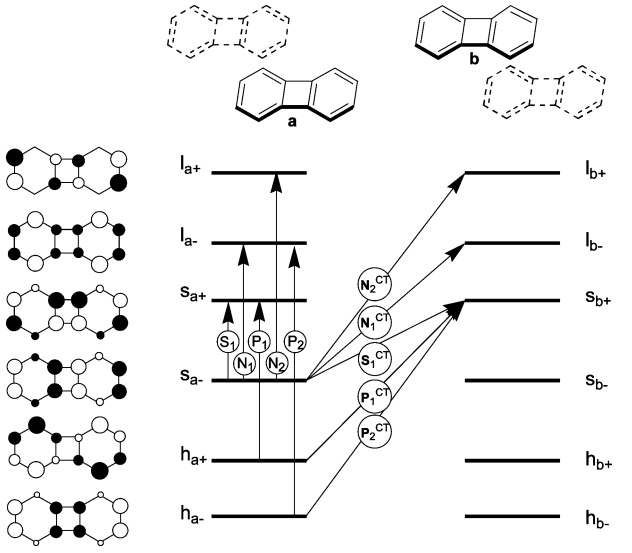

FIGURE 6. Hückel MO's of the J-aggregated biphenylenes, their energies, perimeter labels, and the five singly excited configurations responsible for the S_1, N_1, N_2, P_1, and P_2 states.

TABLE 2. Calculated Electronic Transitions for [2,2]Biphenylenophane in H-Aggregation, the Face-to-Face Arrangement

state	E[a]	f	state function
1	26.96	0	$0.69S_{1-} + 0.15_{1-}{}^{CT}$
2	27.46	0	$0.70S_{1+}$
3	31.02	0	$0.69N_{1+} + 0.12N_{1-}{}^{CT}$
4	31.71	0.19	$0.70N_{1-}$
5	36.67	0	$0.70S_{1+}{}^{CT}$
6	37.09	0	$0.69S_{1-}{}^{CT} + 0.15S_{1-}$
7	40.24	0	$0.52P_{1-} + 0.44N_{1-}{}^{CT} + 0.18P_{1-}{}^{CT}$
8	41.19	0.03	$0.70N_{1+}{}^{CT}$
9	42.33	0	$0.54N_{1-}{}^{CT} - 0.42P_{1-} - 0.14_{1-}{}^{CT}$
10	42.76	0	$0.68N_{2+} - 0.19N_{2-}{}^{CT}$
11	43.54	0.22	$0.70N_{2-} + 0.11N_{2+}{}^{CT}$
12	45.15	3.6	$0.66P_{1+} - 0.24P_{1+}{}^{CT}$

[a] Energy in 10^3 cm^{-1}.

The results of calculations for the biphenylene cyclophane in the two different spatial H-type and J-type aggregations are shown in Tables 2 and 3. The state correlation diagram of these two states between monomer and two types of cyclophanes is shown in Figure 7. The lowest two electronic states of the H-aggregated and the J-aggregated biphyenylenes (states 1 and 2 in Tables 2 and 3) originate from symmetric and antisymmetric

(29) Fleischhauer, J.; Ho1weler, U.; Spanget-Larsen, J.; Raabe, G.; Michl, J. *J. Phys. Chem. A* **2004**, *108*, 3225.

TABLE 3. Calculated Electronic Transitions for [2,2]Biphenylenophane in J-Aggregation, the Head-to-Tail Arrangement[a]

state	E	f	state function
1	27.40	0	$0.70S_{1+}$
2	27.51	0	$0.70S_{1-}$
3	31.45	0	$0.70N_{1-}$
4	31.77	0.23	$0.70N_{1+}$
5	40.79	0	$0.70S_{1+}{}^{CT}$
6	40.80	0	$0.70S_{1-}{}^{CT}$
7	42.22	0	$0.70P_{1-}$
8	43.38	0.04	$0.70N_{2-}$
9	43.59	0	$0.70N_{2+}$
10	44.78	3.84	$0.68P_{1+} - 0.16N_{1+}{}^{CT}$
11	45.42	0	$0.70N_{1-}{}^{CT}$
12	45.46	0.24	$0.68N_{1+}{}^{CT} + 0.16P_{1+}$

[a] Energy in 10^3 cm^{-1}.

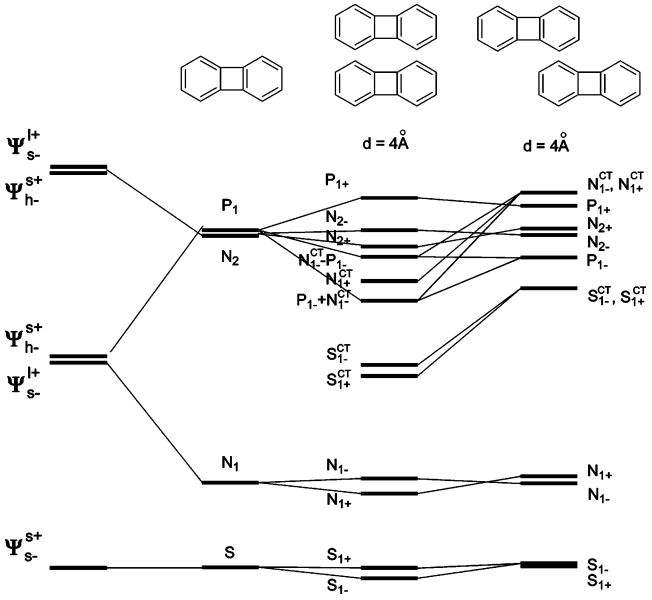

FIGURE 7. State correlation diagrams of biphenylene, H-aggregrated biphylenes, and J-aggregrated biphenylenes.

linear combinations of monomeric $s_- \rightarrow s_+$ local transitions. Both states have vanishing oscillator strength as expected from the null value of corresponding monomeric transitions. The experimental observations of weak fluorescence progression around 530−550 nm are probably due to the vibronic borrowing effect. In addition, the larger overlap between two moieties in the H-type cyclophane with face-to-face arrangement leads to a small mixing of charge-transfer configuration. The exciton coupling between two moieties estimated from the energy splitting between these two states ranges from 0.1 eV (J-cyclophane) to 0.5 eV (H-cyclophane). With such a small exciton coupling, we expect that these two low-lying electronic states exhibit trapped localized excitation in the presence of exciton−phonon coupling.

The next two electronic states (states 3 and 4 in Tables 2 and 3) have their origin as $s_- \rightarrow l_-$ local excitations. These two states consist mostly of delocalized neutral exciton states with almost no charge transfer in the J-type cyclophane with two moieties in head-to-tail alignment. The state with in-phase oscillation of transition dipole of two local excitons (N_{1+} in J-type and N_{1-} in H-type cyclophane) generates small absorption intensity. Hence, we believe that the observed minimal peak of around 370 nm in the experiment is due to this exciation. States 5 and 6 are two degenerate dark electronic states involving symmetric and antisymmetric combinations of charge-transfer configurations from $s_{1-} \rightarrow s_{2+}$ and $s_{2-} \rightarrow s_{1+}$.

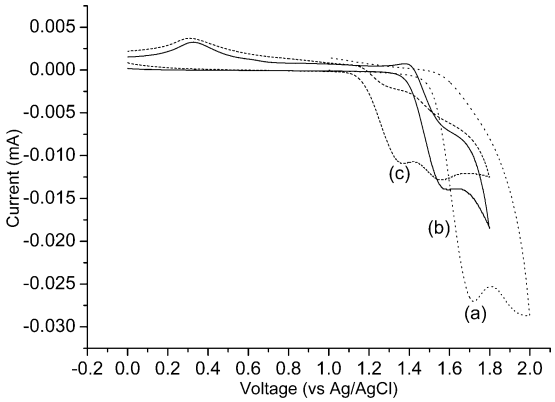

FIGURE 8. Cyclic voltammograms for (a) **9**, (b) **10**, and (c) **4**.

The two electronic states originating from two local P_1 excitations (states 7 and 10 in J-cyclophane; and states 7 and 12 in H-cyclophane) have the largest exciton splittings of 2.56 and 4.91 eV, respectively (Figure 7). This indicates that there exists a strong dipole−dipole coupling between these two moieties. For both arrangements, the delocalized exciton with higher energy carries most of the intensity, which is in agreement with the experimental observation that an intensive absorption around 260 nm is seen. Interestingly, this brightest state of the J-aggregated biphenylenes contains 5% of CT characteristics while the H-aggregated biphenylenes contains 11% of the CT characteristic. This kind of excimeric character of the excited states becomes even more dramatic when the distance between two moieties is closer, for instance, $w_{CT} = 50\%$ when $d = 3.5$ Å in the case of H-type cyclophane. Hidden behind the strong absorption band due to P_{1+}, there are several forbidden and weakly allowed electronic states originating from N_2 and $N_1{}^{CT}$ local states. Detailed discussion of the nature and classification of these electronic states will be presented in another publication.

Redox Behavior of 4. Electrochemistry is another common approach that could be used to evaluate spatial interactions between proximate groups.[3d] π-Orbital overlapping between the biphenylene units may create interchromophore repulsions, leading to a reduction of the oxidation potential. The electrochemical behavior of **4**, **9**, and **10** (1×10^{-3} M) was examined by cyclic voltammetry (CV) for comparison. The CV experiments were carried out on Pt electrodes in CH_2Cl_2 with $(Bu)_4NClO_4$ as the supporting electrolyte and a saturated Ag/AgCl electrode as the reference. Oxidation waves of the authentic samples of biphenylene **9** and [2.2]paracyclophane **10** peaked at 1.72 and 1.59 V also served as references for comparison. Cyclophane **4** showed two irreversible sequential-oxidation waves peaked at 1.37 and 1.55 (Figure 8, line c), indicating that **4** could be oxidized more easily than **9** by 0.22 V and **10** by 0.35 V. Splitting of the oxidation waves indicated that removal of the second electron from **4** is more difficult than the first one. We

tentatively attributed this to the proximity effects of the biphenylene units that lead to electronic repulsion, favoring the first oxidation of the biphenylene units. In addition, electronic delocalization of the positive charge between two biphenylene units may also stabilize the corresponding cation, making the second oxidation more difficult.

Thermal Stability. Upon rising the temperature to 220 °C in high vacuum ($<1 \times 10^{-5}$ Torr), **8** sublimed without any decomposition. In addition, the unsublimed sample of **8** residing in the hot zone of the sublimator was also checked by ^{1}H NMR and proved stable after being heated for hours. The high thermal stability is remarkable in consideration of the high ring strains of **8**.

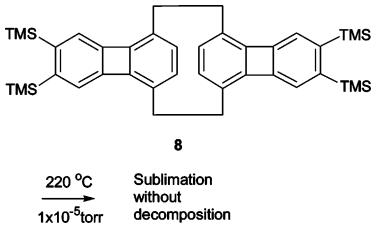

For [2.2]paracyclophane bearing 31−33 kcal/mol of strain energy, cleavage of the ethano bridges is thermodynamically favorable due to ring opening and the release of associated strain,[30] leading to benzyl−benzyl biradicals above 200 °C along with substantial chemical reactions, such as isomerization or racemization.[31] In addition, the unusually long ethano bridges made the C−C bonds kinetically labile toward thermal dissociation.

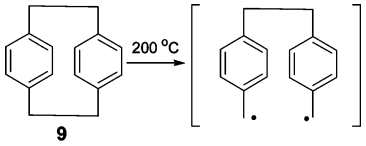

On the contrary, as described in a previous section, the ethano bridges of **4** are less strained than that of **9**, implying that the ethano C−C bonds are stronger and therefore should have better resistance toward homolytic thermal cleavage.

Stanger's theoretical calculations by the hybrid DFT method suggested that conversion of dicyclobutadieno-[2.2]paracyclophane and benzene to [2.2]paracyclophane and benzocyclobutadiene is endothermic by 5.9 kcal/mol.[32,3c]

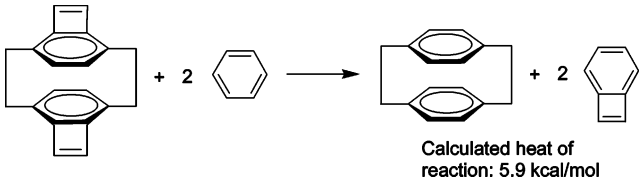

Stanger attributed this observation to the stabilizing interactions between the aromatic moieties and the ethylene bridges and suggested that introduction of the σ-strained four-membered rings into the π-strained [2,2]-paracyclophane is energetically more favored than that into the π-relaxed benzene ring. Since thermal cleavage of the ethano bridges would release the strains on the boat-shape benzenoid rings and give rise to the π-relaxed diradical, one may expect that the presence of the σ-strained four-membered rings would hinder this thermal cleavage. This could reasonably explain the unusual thermal stability of **8** in the present work.

In summary, we have successfully synthesized the highly strained biphenylenophanes **4** and **8** that exhibit salient phane-state delocalization properties. In addition, compound **8** was found to be thermally stable and is able to sublime at 220 °C without decomposition. Studies on the flash vacuum pyrolysis behavior of **4** at high temperatures and the syntheses of the higher [*N*]phenylenophanes are currently in progress.

Experimental Section

General Procedures. Compound **5**[31] and TMSC≡CZnCl[15] were prepared according to literature procedures. CH_2Cl_2 for spectral analysis as well as for cyclic voltammetry was dried over P_2O_5 and distilled before use. Pt working and counter electrodes and an Ag/AgCl reference electrode were used in the electrochemical studies.

4,5,12,13-Tetrakis(trimethylsilyl)ethynyl[2.2]paracyclophane (6). To a two-neck flask were added **5** (0.3 g, 0.57 mmol), $Pd(PPh_3)_4$ (0.4 g, 0.35 mmol), and a solution of TMSC≡CZnCl in dry THF. (Note that the solution of TMSC≡CZnCl in dry THF was prepared according to the following procedure: To TMSC≡CH (0.56 g, 5.71 mmol) in dry THF (5 mL) at −78 °C in a three-neck flask under argon was added 1.6 M *n*-butyllithium solution (4 mL) in THF (5 mL) slowly through an addition funnel, followed by anhydrous zinc chloride (0.9 g, 6.62 mmol) in THF (10 mL) slowly. The reaction mixture was stirred at −78 °C for 1 h and allowed to stir at room temperature for 1 h.) The mixture was refluxed at 70 °C under nitrogen for 4 days. After 2 days of refluxing, additional TMSC≡CH (0.28 g, 2.86 mmol) was added, and refluxing was continued for another 2 days. After addition of 1 N HCl (50 mL), the reaction mixture was extracted with dichloromethane (2×100 mL). The combined organic layer was washed with brine and dried over anhydrous magnesium sulfate. The solvent was evaporated, and the residue was chromatographed on silica gel with 5% dichloromethane in hexane to give **6** as a colorless crystalline solid (0.1 g, 30%): mp 242−243 °C; ^{1}H NMR (400 MHz, $CDCl_3$) δ 6.85 (s, 4H), 3.44−2.89 (m, 8H), 0.30 (s, 36H); ^{13}C NMR (100 MHz, $CDCl_3$) δ142.3, 129.4, 127.6, 103.7, 102.1, 32.4, 0.3; MS *m/z* 593.3 $(M + 1)^+$; HRMS calcd for $C_{36}H_{48}Si_4$ 592.2833, found 592.2830 M^+.

***anti*-(6,6′,7,7′-Tetrakis(trimethylsilyl))[2.2](1,4)biphenylenophane 8.** To tetrakis(trimethylsilyl)ethynyl paracyclophane **6** (0.2 g, 0.34 mmol) in tetrahydrofuran (30 mL) was added excess TBAF (0.9 g, 3.45 mmol) slowly and the mixture stirred at room temperature overnight. To the reaction mixture was added water (40 mL). The product was extracted with dichloromethane (2×100 mL). The combined organic layer was washed with brine and dried over anhydrous $MgSO_4$.

(30) (a) Hopf, H.; Marquard, C. In *Strain and its Implications in Organic Chemistry*; de Meijere, A., Blechert, S., Eds.; NATO ASI Series; Kluwer: Dordrecht, 1998; Vol. 273, pp 297−332. (b) Boyd, R. H. *Tetrahedron* **1966**, *22*, 119−122.

(31) (a) Sankararaman, S.; Hopf, H.; Dix, I.; Jones, P. G. *Eur. J. Org. Chem.* **2000**, 2703−2709. (b) Sankararaman, S.; Hopf, H.; Dix, I.; Jones, P. G. *Eur. J. Org. Chem.* **2000**, 2711−2716. (c) Hopf, H.; Kleinschroth, J. *Angew. Chem., Int. Ed. Engl.* **1982**, *21*, 469−480. (d) Truesdale, E. A.; Cram, D. J. *J. Org. Chem.* **1980**, *45*, 3974−3981. (e) Sato, T.; Torizuka, K.; Shimizu, M.; Kurihara, Y.; Yoda, N. *Bull. Chem. Soc. Jpn.* **1979**, *52*, 2420−2423. (f) Shono, T.; Ikeda, A.; Hayashi, J.; Hakozaki, S. *J. Am. Chem. Soc.* **1975**, *97*, 4261−4264. (g) Reich, H. J.; Cram, D. J. *J. Am. Chem. Soc.* **1967**, *89*, 3078−3080; **1969**, *91*, 3517−3526. (h) Helgeson, R. C.; Cram, D. J. *J. Am. Chem. Soc.* **1966**, *88*, 509−515.

(32) Stanger, A.; Ber-Mergui, N.; Perl, S. *Eur. J. Org. Chem.* **2003**, 2709−2712.

Solvent was carefully evaporated by rotary evaporator under reduced pressure to give a pale brown crystalline solid **7** (0.092 g, 90%): ^{1}H NMR (400 MHz, $CDCl_3$) δ 6.93 (s, 4H), 3.48 (s, 4H), 3.48−3.00 (m, 8H); ^{13}C NMR (100 MHz, $CDCl_3$) δ 143.0, 130.2, 127.2, 84.7, 81.9, 32.3.

A solution of tetrayne **7** (0.055 g, 0.2 mmol) and TMSC≡CTMS (0.14 g, 0.82 mmol) and dicarbonylcyclopentadienyl cobalt (0.05 mL, 0.4 mmol) in dry toluene (20 mL) was added to boiling TMSC≡CTMS (0.13 g, 0.76 mmol) in toluene (20 mL) through a syringe pump over a period of 4 h while being irradiated with a halogen lamp (125 W, 120 V) at a distance of 4 cm from the center of the reaction flask. Irradiation was continued for 10 h at reflux after addition was complete. The reaction mixture was cooled, and the solvent was distilled by short-path distillation. The dark residue was chromatographed on neutral alumina with 5% dichloromethane in hexane as eluent to give a yellow crystalline solid **8** (39 mg, 34%): mp 298−299 °C; ^{1}H NMR (400 MHz, $CDCl_3$) δ 6.92 (s, 4H), 5.86 (s, 4H), 2.86−2.70 (m, 8H), 0.35 (s, 36H); ^{13}C NMR (100 MHz, $CDCl_3$) δ 152.9, 148.5, 147.0, 131.8, 131.1, 122.4, 30.9, 2.5; MS (FAB) *m/z* 644.3 (M^+); HRMS (FAB) calcd for $C_{40}H_{52}Si_4$ 644.3146, found 644.3145 (M^+); UV−vis λ_{max} (nm) 281 (ϵ = 127000), 362 (ϵ = 8500), 385 (ϵ = 7100).

***anti*-[2.2](1,4)Biphenylenophane (4).** To biphenylenophane **8** (9 mg, 0.014 mmol) in dry THF (2 mL) was added TBAF (80 mg, 0.31 mmol) and the mixture stirred overnight at room temperature. To this reaction mixture was added trifluoroacetic acid (1 mL) and the resulting mixture stirred for another 2 h. The reaction mixture was quenched with water (30 mL) and extracted twice with dichloromethane (2 × 50 mL). The organic layer was washed with water and brine and dried over anhydrous magnesium sulfate. Removal of solvent and column chromatography with neutral alumina, using 20% CH_2Cl_2/hexanes as the eluent, gave the yellow crystalline solid **4** (3 mg, 60%): mp 281−282 °C; ^{1}H NMR (400 MHz, $CDCl_3$) δ 6.75 (AA′ m, 4H), 6.64 (BB′ m, 4H), 5.92 (s, 4H), 2.85−2.68 (m, 8H); ^{13}C NMR (100 MHz, $CDCl_3$) δ 151.7, 149.5, 131.6, 131.2, 127.7, 117.1, 30.6; MS (FAB) *m/z* 356.4 (M^+, 15), 177.8 (100), 176.0 (85), 152.1 (36); UV−vis λ_{max} (nm) 259 (ϵ = 84300), 357 (ϵ = 5800), 379 (ϵ = 5300). The structure was further confirmed by X-ray crystallographic analysis.

Acknowledgment. We thank the National Science Council of Republic of China for the financial support (NSC 92-2113-M-002-020).

Supporting Information Available: ^{1}H and ^{13}C NMR spectra of **4**, **6**, **7**, and **8** and NOESY of **6** and **8**; CIF data and the ORTEP for **4**; and the *XYZ* coordinates for the biphenylene structure used in the calculation. This material is available free of charge via the Internet at http://pubs.acs.org.

JO047802N